

# The study of flow type dynamics at pedon scale via morphometric parameter analysis of dye-pattern profiles

Juraj Bebej<sup>1\*</sup>, Tomáš Orfánus<sup>2</sup>, Marián Homolák<sup>1</sup>, Meni Ben-Hur<sup>3</sup>, Viliam Pichler<sup>1</sup>, Jozef Capuliak<sup>4</sup>

<sup>1</sup> Technical University in Zvolen, Faculty of Forestry, Department of Natural Environment, T. G. Masaryka 24, 960 53 Zvolen, Slovakia. E-mails: marian.homolak@tuzvo.sk, viliam.pichler@tuzvo.sk

<sup>2</sup> Institute of Hydrology, Slovak Academy of Sciences, Dúbravská cesta 9, 841 04 Bratislava, Slovakia. E-mail: orfanus@uh.savba.sk

<sup>3</sup> Institute of Soil, Water and Environmental Sciences, The Volcani Center, Agricultural Research Organization, P.O. Box 6, Bet Dagan, 50–250, Israel. E-mail: meni@volcani.agri.gov.il

<sup>4</sup> National Forest Centre, T. G. Masaryka 22, 960 92 Zvolen, Slovak Republic. E-mail: Jozef.Capuliak@nlcsk.org

\* Corresponding author. E-mail: juraj.bebej@tuzvo.sk

**Abstract:** The application of Brilliant Blue FCF tracer enables to identify flow types in multi-domain porous systems of soils via analyses of morphologic parameters of stained objects occurring in dye pattern profiles, as they represent the footprint of flow processes which occurred in soil during both the infiltration and the redistribution of dye solution. We analysed the vertical dye pattern profiles exposed for different time lengths, and revealed temporal evolution of dye solution redistribution leading to changes in flow types. The field experiment was performed with the Brilliant Blue tracer (the 10 g l<sup>-1</sup> concentration) applied on 1m x 1m surface of the Dystric Cambisol. The top litter horizon had been removed before 100 l of the tracer was applied. Four vertical profiles were excavated on the experimental plot (always 20 cm apart) at different times after the irrigation had been finished: 2 hours (CUT 2), 24 hours (CUT 24), 27 hours (CUT 27) and 504 hours (CUT 504). The analyses of the dyed patterns profiles showed the spatio-temporal changes in the dye coverage, surface area density, average BB concentration, and stained path width, which allowed us to specify three stages of dye solution redistribution history: (i) a stage of preferential macropore flow, (ii) a stage of strong interaction between macropore-domain and soil matrix leading to the generation of heterogeneous matrix flow and fingering flow types, and (iii) a final stage of dye redistribution within the soil body connected with leaching of BB caused by meteoric water. With increasing time, the macropore flow types convert to mostly matrix-dominated FTs in the upper part of the soil profile. These results were supported by soil hydrological modelling, which implied that more than 70% of the soil moisture profiles variability among CUT 2–CUT 504 could be explained by the time factor.

**Keywords:** Dye pattern; Preferential flow; Flow types; Image analysis; Morphometric parameters; Spatio-temporal flow of dye solution.

## INTRODUCTION

Dye tracing has become an established way to demonstrate the preferential flow of water in soil and its spatial patterns within soil profiles (Allaire et al., 2009; Capuliak et al., 2010; Flury et al., 1994; Garrido et al., 2014; Ghodrati and Jury, 1990; Vogel et al., 2007). The dye solution transfer in soils can be evaluated by image analysis (Forrer, 2000), which enables to identify the dye solution flow pathways in soils, to measure the morphometric parameters of stained objects, and finally, to determine the flow types (FT) within the observed dye solution pathways (Weiler, 2001; Weiler and Flühler, 2004).

The preferential flow as a specific kind of water transport in soil is defined as the rapid downward transport of water and solutes via preferred pathways through porous medium (Jury and Horton, 2004). The preferential flow involves rapid flow through large pores termed macropores, that are ubiquitous in structured soils, funnel flow or heterogenous flow (Kung, 1990) and unstable fingered flow (Ritsema and Dekker, 2000), as they arise from distinctively different physical processes (Jury and Horton, 2004). In soils, the above mentioned preferential flow types may occur in tandem, or in the absence of some of them (Jury and Horton, 2004).

Direct measurement of mutual relationships of individual preferential flow types present in field soils is rather difficult because of the tremendous spatial and temporal variability of flow pathways. Tracing with mobile dye is also difficult,

because excavation of soil is destructive and experimental results cannot be repeated at the same location (Flury et al., 1994). In consequence, the analysis of dye flow pathways in soils is usually limited to a sole vertical dye pattern soil profile, excavated for 12 or 24 hours after the dye solution application on experimental plots (Bogner et al., 2012; Bundt et al., 2001; Flury and Flühler, 1994; Flury et al., 1994; Garrido et al., 2014; Hagedorn and Bundt, 2002). In this manner obtained dye pattern profiles represent the snapshots of dye flow pathways in the form of 2-D pictures of 3-D subsurface flow pathways of mobile dye at the time of soil profile excavation. Bundt et al. (2001) excavated a series of five consecutive soil profiles at 10 cm spacing from each other, Alaoui and Goetz (2008) excavated 6 consecutive vertical profiles located 0.20 m apart, Flury et al. (1994) analysed two dye pattern profiles, and Weiler and Flühler (2004) four or five parallel vertical soil sections of 1m x 1m, while the spacing between the vertical sections was 5–7 cm. The analytical outputs obtained by processing such data enable to calculate the spatial variation of the morphometric parameters of dye pattern soil profiles, and/or to calculate the transport of chemical components around preferred pathways using statistical modelling with regard to spatial soil heterogeneity (Bogner et al., 2012). However, in fact, such data reveal spatio-temporal (not only spatial) variability of the dye patterns.

In consideration of this fact, no field study has tackled with the analyses of dye pattern profiles excavated within one soil pedon at different times. Such a study could have revealed the

dynamic processes of dye solution transport in multimodal and spatially heterogeneous porous body of soil pedon using currently available methods for studying dye pattern profiles.

The problem of the current understanding of water transport in the soil can be seen in the following. The preferential flow, especially in the case of macropore flow, is understood as a temporally and spatially stable flow within the macropore structures (e.g. Bogner et al., 2012). On the other hand, the concept of dynamic dye solution flow says that the macropore preferred flow can be limited for a short period, e.g. when the vertical water flow rates are large in relation to the lateral losses into the surrounding soil matrix due to the prevailing pressure potential gradient either at the soil surface, or the nearly saturated subsurface (Li and Ghodrati, 1997; Weiler, 2005). In the case the water entry pressure decreases, the lateral water flow from the macropore into the surrounding soil matrix increases, the macropore flow will terminate and the soil-matrix water flow becomes dominant (Jarvis and Dubus, 2006; Weiler and Flühler, 2004).

At present, very different approaches exist to parameterise dye pattern profiles based on the measurements of stained object characteristics (Bargués Tobella et al., 2014; Droogers et al., 1998; Perret et al., 1999; Ohrstrom et al., 2002; Shipitalo and Butt, 1999; van Schaik, 2009; Zehe and Flühler, 2001). The approach proposed by Weiler (2001), based on the measurements of the volume and density of stained objects, resulted in the classification of flow types, taking into account different intensity of dye solution-soil interaction, too. The biggest advantage of Weiler (2001) classification of flow types is that this classification is supported by experimental research, results of laboratory modelling, as well as field experiments (Weiler and Flühler, 2004; Weiler and Naef, 2003), which ended in the elaboration of an infiltration model flow variability in macropores (Weiler, 2005).

Our objective was (i) to test the spatio-temporal framework of the dye solution hydrodynamics via the morphometric parameter analyses and flow types identification within the soil profiles excavated at different times, (ii) to analyse mutual relationships between the observed flow types and the outputs of hydrological modelling to examine the pedohydrological similarity concept, and, (iii) based on the obtained results to reconstruct the processes of dye solution infiltration and redistribution within the investigated pedon in a complex spatio-temporal framework.

## MATERIALS AND METHODS

### Description of the experimental site

The research was performed at Panský diel (N 48° 48' 25.76'', E 19° 09' 20.47'') in the Starohorské Vrchy Mts., a part of the Western Carpathians (Mazúr and Lukniš, 1980), Slovakia, at an

altitude of 910 m a.s.l. This area is covered by a 90-year old mixed forest of Norway spruce (*Picea abies* (L.) Karst.), a dominant species, silver fir (*Abies alba* Mill.), European beech (*Fagus sylvatica* L.), Weymouth pine (*Pinus strobus* L.) and European larch (*Larix decidua* Mill.). The experimental plot was located on a flat area with negligible inclination, and its geology contained complexes of sediments formed from schist, acidic granitites, arkoses, greenish and reddish mica-slates and quartzite (Andrusov et al., 1985). These rocks were also the forming substrate of the local soil. The climate in the experimental plot is from moderately warm, humid to moderately cold with mean annual temperature of 4.1°C and mean annual precipitation total of 1.023 mm. The soil in the experimental plot is *Dystric Cambisol* (IUSS Working Group WRB, 2015), and its profile description is presented in Table 1.

### Experiment Setup

A detailed geophysical survey of the experimental plot area by electric resistivity tomography (ERT) revealed sudden, mosaic changes of hydrophysical properties of soils in the surroundings of the experimental plot, reflecting the changes in both the soil textures and the soil types other than *Dystric Cambisol*, as well as in mineralogical changes of soil skeleton and its volume abundances within the soil profiles (Fig. 1).

These circumstances had direct impacts on the originally considered design of experiment, as these made it impossible to carry out the experiment on several plots with replications. In order to overcome this obstacle, we proceeded to conduct our field experiment only on one experimental plot, via intensively oriented research, based on the comprehensive study of dye solution transport in soil pedon, via utilisation of various and mutually independent methods of study, as specified below.

The air temperature and precipitation at the experimental plot were monitored by an automatic station of the EMS Brno Company (Czech Republic) - Fig. 2. Potential evapotranspiration (PET, mm h<sup>-1</sup>) was calculated using Penman equation (Penman, 1948).

No rainfall was observed during the period between the BB application and excavation of CUT 2, CUT 24, and CUT 27, but several rainfalls were recorded between CUT 27 and CUT 504 excavation (Fig. 2).

In April 30, 2012, Brilliant Blue (BB) FCF dye solution with 10 g l<sup>-1</sup> concentration was applied by a sprinkler with 100 mm h<sup>-1</sup> intensity over a 1 m x 1 m plot. High concentration of dye tracer (BB) was applied to eliminate dye retardation (Kasteel et al., 2002), as well as to increase the visual resolution of stained objects of dye pattern profiles.

The sprinkler consisted of a board supporting 1,600 needles with a 0.5 mm diameter arranged in a 40 x 40 grid. Each needle was individually connected to a liquid distribution vessel

**Table 1.** Description of soil profile in the experimental site.

	Soil horizons	(cm)	Soil horizon description
Forest-floor litter horizon O <sub>o</sub>	Sub-horizon O <sub>oi</sub>	1.5–7.0	Broad-leaf and needle litter (with sprays, cones...)
	Sub-horizon O <sub>of</sub>	0.5–1.5	Moderately decomposed plant litter
	Sub-horizon O <sub>oh</sub>	0.0–0.5	Strongly decomposed plant litter
	Horizon Au	0–5.0	Umbric, dark brown, sandy loam, wet, loose with slightly nodular structure, with gravel content of approximately 5 %, moderately rooted, apparent transition to Bv horizon
	Horizon C <sub>1</sub>	110 +	Light brown, sandy, wet, compacted.
Subsurface horizons	Cambic B <sub>v</sub> horizon	5–110	Brown (HUE 5YR, Value 4, Chroma 4) from the upper part tongue-like spots of purplish tone (HUE 5 YR, Value 3, Chroma 3), loamy sand, slightly wet, compacted (less where purple), moderately rooted – slightly in a lower part, gradual transition to C <sub>1</sub> .
	Horizon C <sub>1</sub>	110 +	Light brown, sandy, wet, compacted.

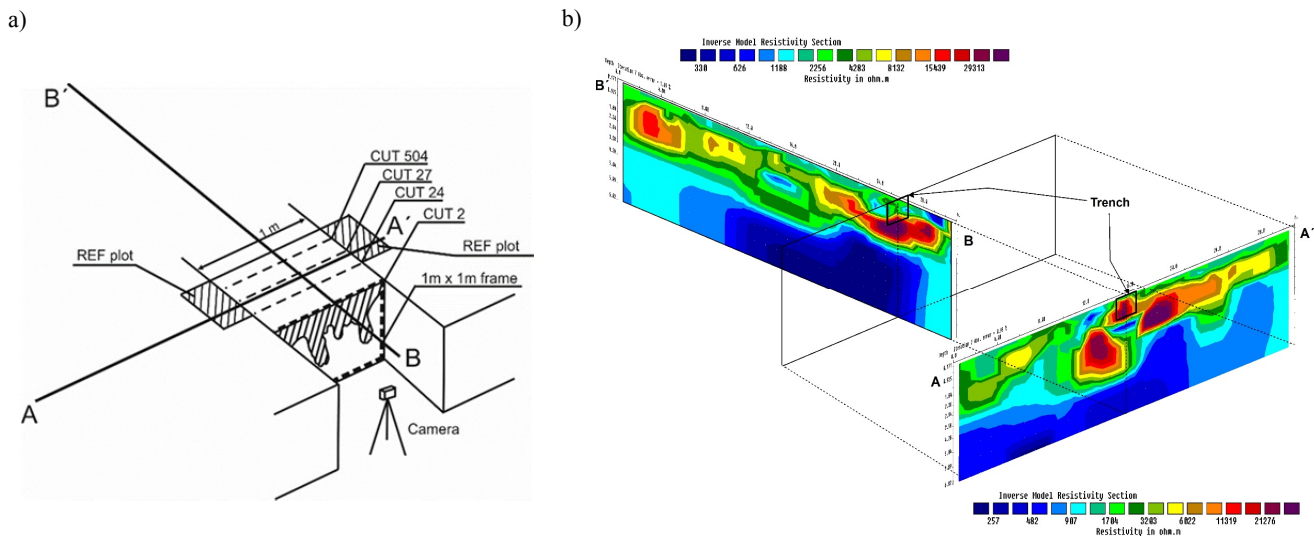


**Fig. 1.** The location of both the experimental and the REF with projection of CUT2 – CUT 504 soil profiles (a). The lines A-A' (the contour line), and B-B' (fall line) represents the orientation of ERT profiles (b), which show the subsurface structures of coloured slates with high electrical resistivity values (11 000–30 000  $\Omega\text{m}$ ) floating on slope deposits with low electrical resistivity values (300–1000  $\Omega\text{m}$ ) (dipole-dipole array).

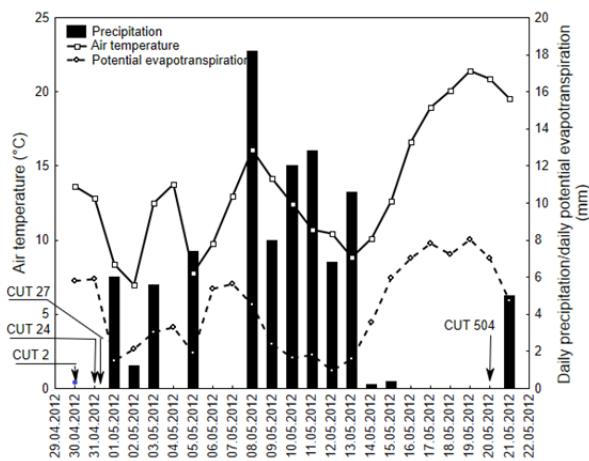


**Fig. 2.** Temperature, potential evapotranspiration and precipitation at the experimental site.

through the plastic tubings. The tank was supplied with dye solution by a piston diaphragm dosing pump (DME 150, Grundfos Alldos, Reinach, Switzerland) operating in the range of  $0.1\text{--}140\text{ l h}^{-1}$  with negligible pulsation. The board supporting needles had an industrial vibrator attached to it to assure uniform distribution of droplets over the experimental plot.

We irrigated continuously for 1 hour, so the flooding regime of irrigation was achieved. The tree litter and duff were cleared before irrigation, as organic horizons may have significant influence on flow patterns (Capuliak et al., 2010), as well as on macropore flow initiation process.

As the experimental plot was located on a flat area of the hillslope, the lateral outflow of dye solution from the experimental plot was prevented, and only vertical infiltration of dye solution took place.

After the BB application, a series of four vertical profile cuts,  $1\text{ m} \times 1\text{ m}$  each, were excavated at different times, namely after 2 (CUT 2), 24 (CUT 24), 27 (CUT 27), and 504 hours (CUT 504), revealing the dye pattern profiles for further analysis (Fig. 1). The soil profiles were photographed with a digital camera (Canon EOS 450D) mounted on a stable tripod. Before photographing, the  $1\text{ m} \times 1\text{ m}$  gray frame with a ruler was mounted on the soil

profile faces to prevent a geometrical distortion and to assure inhomogeneous illumination correction. The obtained pictures were recorded and stored in the raw format. Afterwards, the sample-extraction sites within the domain of particular profiles were marked, and the profiles were photographed again.

The individual CUT profiles were spaced 20 cm apart, with CUT 2 positioned about 20 cm from the trench bank and the other CUTs were excavated sequentially to the trench front (face uphill). In order to eliminate the dye pattern edge effect, the edge sections of the profiles were excluded from sampling.

The times of excavation events were selected according to the following rules: standard excavation time was considered as 24 hours (CUT 24), the time of 2 hours (CUT 2) was selected to document the dye pattern profile evolved during the infiltration stage (i.e., in time, when thin film of dye solution still remains on the top of irrigated area). The 27-hour profile (CUT 27) was excavated in order to evaluate potential changes in dye pattern profile shortly after standard excavation time (24 hours), when redistribution of dye solution in soil was dominant process in soil pedon. Such an approach enables to access the changes in dye pattern profiles, which emerged during both, the infiltration (CUT 2) and the redistribution stage (CUT 24 and CUT 27) of the dye solution flow in soil profile. The excavation time of the CUT 504 was chosen to record the potential changes in dye pattern as affected by meteoric water imbibition.

After the excavation of CUT 504, additional two vertical profiles were excavated ( $1\text{ m} \times 0.5\text{ m}$  each), 35 cm next to the both, left and right edges of the  $1\text{ m} \times 1\text{ m}$  experimental plot. No BB tracer had been applied on the soil surface in this case. These plots are referred as REF (“reference”) plots in our study (Fig. 1). The REF profiles served for the comparison with CUT 2 – CUT 504 profiles to reveal physical and chemical changes induced by Brilliant Blue dye solution.

As mentioned, in order to overcome the obstacles resulting from the spatial heterogeneity in soil in the vicinity of the experimental plot area, we proceeded to conduct our field experiment via utilisation of different and mutual independent methods of study:

- Soil reactions changes: It can be expected, that irrigation of acidic soils ( $\text{pH} < 4.0$ ) with abundant BB dye solution ( $\text{pH} = 7$ ) would change the  $\text{pH} (\text{H}_2\text{O})$  values of soil samples on

experimental plot significantly. The intensity of such changes can be judged by comparing them with soil reaction profiles from the REF plots, unaffected by dye solution. With respect to spatio-temporal evolution of the dye infiltration/redistribution process within soil pedon, the temporal changes in soil reaction profiles should be revealed in soil profiles excavated at different times.

- **Chemical changes:** The sodium represents 5.8% of BB FCF dye molecule weight component; therefore, sodium represents an important agent applied into the soil during the irrigation experiment. The changes of  $\text{Na}^+$  concentration ( $\text{cmol}_c \text{ kg}^{-1}$ ) in the soil exchangeable complex inside the irrigated part of the pedon (when compared to  $\text{Na}^+$  ( $\text{cmol}_c \text{ kg}^{-1}$ ) in REF plots) should follow the spatio-temporal redistribution of the dye-solution in the soil pedon in a similar way, as was the case of soil reaction.

- **Interaction changes:** The process of water transport into the surrounding matrix is referred to as lateral infiltration, or interaction (Weiler and Flühler, 2004; Weiler, 2005). The interaction processes are controlled by water supply into macropores, flow conditions in the macropores and by water transport from macropores into the surrounding matrix (Beven and Germann, 1982; Weiler, 2005). In the case when soil profiles excavated at different times record the spatio-temporal process of dye solution infiltration/redistribution in the soil pedon, the  $c \text{Na}^{+(\text{IC})} / c \text{Na}^{+(\text{NC})}$  ratio should reveal the interaction changes between the intensely coloured zones of macropore flow (IC zones) and the surrounding soil matrix of less coloured zones ("soil matrix" – NC zones).

The sampling procedure was adapted to meet the set objectives defined for physical-chemical analyses. Three samples from each 10 cm layer of each CUTs of the experimental plot were taken by Kopecky-cylinder with volume of  $100 \text{ cm}^3$ , with consideration of colouring intensity: samples labelled as NC (from sites not affected by BB dye), MC (taken from zones with moderate colouring) and IC (samples intensively coloured by BB dye solution). In total, 120 soil samples were taken for physical and chemical analysis from CUT 2 - CUT 504 soil profiles. The soil samples were taken also from the REF plots, where two samples were taken from each 10 cm layer, i.e. in total 20 samples were taken from REF zones.

The results of all above mentioned independent and indirect methods of dye solution flow were summarised and evaluated by Bebej et al. (2017). It was also found that according to the USDA soil taxonomy, the soil samples taken from both the experimental and the REF plots were classified as sandy clay loam (usually, samples from 0.1 to 0.5 m depth), and sandy loam (samples below 0.5 m), and no significant texture differences were found between the experimental and the REF plots. On the other hand, the statistical analysis showed that the depth influenced the percentage content of clay with very high significance ( $p = 0.000$ ) in all soil profiles, and that the lowest clay content was in 100 cm depth. According to the statistical tests, the colouring intensity was significantly related to particle-size distribution, especially to sand fraction, since its content in the intensively coloured zones was significantly higher than in the non-coloured zones ( $p = 0.000$ ). The silt content in the intensively coloured zones was significantly lower than in the samples from the moderately coloured zones ( $p = 0.000$ ), or from the non-coloured zones ( $p = 0.001$ ). It was found that the skeleton content increased with the depth, reaching its maximum in depth interval of 0.4–0.7 m. Generally, no significant differences in the skeleton content were observed among the individual profiles of both, the experimental and the REF plots. From the mineralogical point

of view, the soil skeleton is represented by clasts of extremely acid quartzites, sandstones, gray-green-, and red-coloured mica slates. The silicate analyses of fine earth soil samples taken from the soil profiles of REF plots showed no differences in chemical and mineralogical composition of soil. Considering the skeleton composition, its volumetric content, soil textures and chemical composition of fine earth we can propose that the working hypothesis about the spatial representativeness of soil pedon body within the REF and the experimental plots is valid, and that the observed changes in dye pattern profiles will minimally reflect spatial variations existing within the pedon body under investigation (Bebej et al., 2017).

The morphometric parameters chosen for the study of spatio-temporal dye solution transport is based on the measurement of extent and distribution of stained objects within vertical dye pattern profiles excavated at different times (CUT 2 – CUT 504), which can be used for deriving of flow regime characteristics within it. Weiler and Flühler (2004) classified flow processes into five different flow types (FTs), of which three represent the macropore domain, and two the soil matrix FTs. We suppose that predominant flow processes can be deduced from the stained path width (SPW) of stained objects, while SPW limit  $< 20 \text{ mm}$  represents flow pathways, where the dye solution flows primarily in macropores, with minor penetration into the surrounding matrix. In this way, the SPW vertical dye pattern profiles characterised by particular SPW length classes ( $< 20 \text{ mm}$ ,  $20\text{--}200 \text{ mm}$ ,  $> 200 \text{ mm}$ ) can provide information about both, the dominant types of the dye solution flow, and the intensity of macropore-matrix interaction.

The methodology of flow types determination based on SPW evaluation is usually applied without differentiating between the concentration of Brilliant Blue in stained objects. We suggest, that concentration changes should be detected, if the dyed pattern profiles are developing in time.

Specific aspect of our small-scale field experiment relates to the soil water content (SWC) issue. The movement of sorbing solute (Brilliant Blue) is retarded relative to the water flow, because of the partitioning of the solute between the liquid and the solid phases (e.g., Kasteel et al., 2002). The transport processes of dye solution within the soil pedon makes the concentration of Brilliant Blue to be diluted in time course (Germán-Heins and Flury, 2000), and via chromatographic separation of the tracer, the SWC concentration in macropore – soil matrix (i.e. two-domain) system will not spatially coincide with the spatial arrangement of coloured zones. On the other hand, SWC distribution around the zones of preferential flow, and the SWC changes observed in dye pattern profiles exposed at different times, could provide an independent insight on the processes of dye solution flow in the pedon under investigation.

Hydrological modelling (here the HYDRUS dual permeability model) can help to verify the assumption about the temporal dynamics of dye solution transfer processes at the pedon scale. The water balances calculated by the hydrological model include the matrix water content changes, the volumes of water within the fracture domain and the sum of the fluxes on domain boundaries. In our study, the calculated temporal changes of water solution balance can help to understand the dominant macropore flow initiation within the CUT 2 profile (see also Li and Ghodrati, 1997; Weiler and Naef, 2003). In the case of macropore flow initiation on soil surface (CUT 2), the total water content changes in the soil matrix of CUT 2 profile should be very low, because of water bypassing the soil matrix via macropores. By flow initiation theory (Weiler, 2005), an extremely high outflow of dye solution via macropore network should be observed.

## Data processing

### Evaluation of dye concentration in soil

To calibrate the images for the concentration of BB from the stained flow region, 10 small disturbed soil samples of one to three grams were scraped off the surface of soil profiles from various depths. The sample locations were marked and the soil profile was photographed the second time. The BB concentrations were obtained by extracting BB in the laboratory as described in the following section.

To calibrate the relationship between the colour coordinates and BB concentration, the scraped soil samples were dried at 80°C for 24 hours. From each homogenised soil sample, a sub-sample of 0.5 g was weighed in an extraction column (8 ml, empty, glass with PTFE frits), and put in a vacuum vessel. Ten ml of a solution with 4:1 (v : v) ratio of water : acetone was added as an extraction solvent, and the vessel was vapourised under low pressure of ~ -600 Pa for one hour. The extract was filtered through a 0.45 µm filter, the BB concentration in the extract was measured spectrophotometrically (Schimazu UV-1800 Spectrophotometer) at a wavelength of 630 nm (Capuliak, 2008; Capuliak et al., 2010), and the BB concentration in the soil (w : w, BB : soil) was calculated. Based on the calibration graph, dye concentration (C) was calculated for every pixel of the soil profile image and the stained area. For further evaluations, relative dye concentration ( $C_{rel}$ ) as the ratio between C concentration and the approximate dye concentration of 10 g l<sup>-1</sup> ( $C_0$ ) calculated from the dissolution of the total dye tracer amount in 100 l of water used for irrigation.

After taking digital photographs of individual profiles, several procedures were performed to evaluate the spatial concentration of BB in the soil (Forrer et al., 2000): (i) geometric correction; (ii) white-balance and exposure correction; (iii) calibration; (iv) evaluation of the dye concentration. To evaluate the spatial distribution of the various flow types (FTs) in each cut, which was stained by BB, the processing framework in GNU R (R Development Core Team) and C with the help of the ImageMagick image processing library and with a resolution of 500 x 1,000 pixels (i.e., one pixel represents 1 mm x 2 mm) was used (Capuliak et al., 2010).

### Morphometric parameter analyses

Two basic parameters describe the morphology of stained objects in space: the volume density ( $V_v$ ) and the surface area density ( $S_v$ ). The  $V_v$  corresponds to dye coverage ( $D_c$ ) described by Eq. (1) (Flury et al., 1994):

$$D_c = \left( \frac{D_a}{D_a + ND_a} \right) \cdot 100 \quad (1)$$

where  $D_a$  is the surface area in the cut that was stained by dye, and  $ND_a$  is the unstained surface area in the cut.

The  $V_v$  value represents the total sum of the lengths (L) of stained objects, which are equal to the fraction of pixels ( $P_p$ ) filled with stained objects in a particular depth determined with a 1-mm step on the depth axis. In doing so, the total count of the pixels divided by the profile width (1,000 pixels) represents the dye coverage for a given depth (Weiler and Flühler, 2004). The increase of the  $V_v$  ( $D_c$ ) value indicates the growth of the macropore: soil matrix interaction (Weiler and Flühler, 2004), too. Hence, volume density values give first impressions of the differences and similarities of the dye patterns between different experimental sites (Weiler and Flühler, 2004), and between

the dye pattern profiles exposed to a dye tracer in a given experimental plot for different times.

The  $S_v$  value of the profile was estimated from the intercept density calculated as the number of intercepts between the unstained and stained pixels per depth (Weiler and Flühler, 2004).

The  $V_v$  and  $S_v$  values as functions of the soil depth should be interpreted together, because for a given soil depth in a certain soil profile, the  $V_v$  and  $S_v$  values can be different. For example, both the  $S_v$  and the  $V_v$  can be low if small stained areas have also a small surface. However, the  $V_v$  can be high and the  $S_v$  can be low, if the stained object covering the whole soil volume has a small surface (Weiler and Flühler, 2004).

A stained path width (SPW) represents the width of stained flow pathway in the stained object. For each vertical dye pattern, the SPW profile can be calculated as a frequency distribution of three size categories of SPW, <20 mm, 20–200 mm, >200 mm. On the base of the proportion of these SPWs categories, as well as the classification rules of Weiler and Flühler (2004), flow types (FTs) can be distinguished. The mutual relationships among the particular stained object morphometric parameters is presented in Fig. 3.

In order to analyse the spatio-temporal processes of dye solution infiltration and redistribution in soil profiles of the experimental plot, a semi qualitative evaluation of the  $V_v$ ,  $S_v$ , SPW,  $C_{rel}$  and the FTs was used as BB dye solution flow during dye solution infiltration and its redistribution in soil profiles should induce the changes in the  $V_v$ ,  $S_v$ , SPW,  $C_{rel}$  and FT depth profiles regarding local maxima and minima values of the discussed parameters. Consequently, high  $V_v$ , high  $S_v$ , and high SPW class >200 mm designate high values of these parameters at a given depth of the soil profile, and the terms high, low, and average indicate visually observed deviations of the particular values from the values recorded in other dye pattern profiles.

### Mathematical modelling of soil water content profiles

The rationale for the mathematical simulation of the measured soil water profiles using one single set of hydraulic parameters for each horizontal soil layer was to verify the key assumption of the study, namely that the observed changes within dye patterns of four profiles exposed at different times are rather a result of temporal dynamics of dye solution redistribution processes and succession of various flow types than an intrinsic spatial heterogeneity of the soil pedon. If the evaluated pedon could be considered hydraulically homogeneous in this sense, it should be possible to simulate successfully the SWC profiles at any time with one single set of parameters for each defined soil layer.

Soil water content measurements were performed by a gravimetric method (each 10 cm depth 3 measurements). The parameters of soil hydrophysical characteristics of the matrix domain were estimated from the measured soil water retention curves in pressure chambers (Eijkelkamp, The Netherlands) and saturated hydraulic conductivities estimated by a constant head method on the undisturbed samples (Kopecky cylinders) taken from the profile CUT 2. Then the SWC profile created by averaging of values in particular soil depths in CUT 2 was used to solve the inverse problem for the two-domain (dual permeability) environment to calibrate the parameters of the fracture domain. Once calibrated, the parameters were considered same for all other profiles assuming hydrogeological similarity of the soil pedon.

The review of models describing non-equilibrium and preferential flow and transport in the vadose zone has been given e.g. by Šimůnek et al. (2003) and Gerke (2006). While the

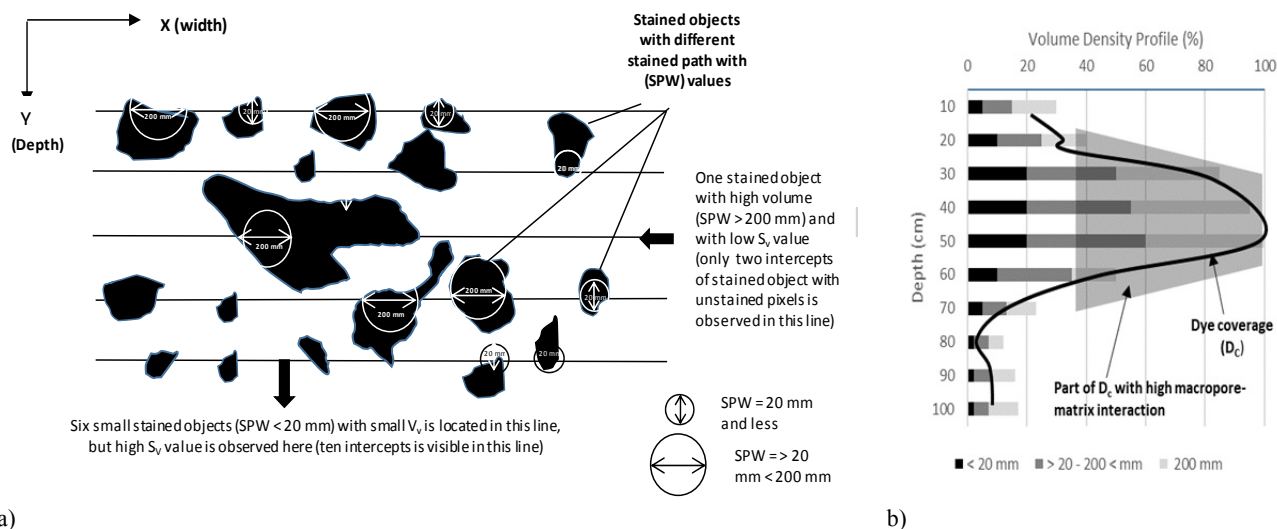


**Fig. 3.** The stained object width measurements in particular vertical sections (Y) provides the information about the  $V_v$ , the  $S_v$  and the stained path width (SPW) distribution of dye pattern profile (a), which are reflected in the formation of  $D_c$  curve, within which a zone with high macropores - soil matrix interaction can be identified, (b).

single-domain model describes the uniform flow in soil porous media, the dual-permeability model can represent a non-equilibrium/preferential flow in a complex system of soil aggregates (matrix) and intermediate spaces (fractures or macropores). In both cases Richards' equation is used to describe the flow in a variably saturated rigid porous medium for one-dimensional isothermal Darcian flow. While in the case of a single-porosity system the Richards' equation is solved for the entire flow domain, in the dual-permeability model, it is applied separately to each of the two pore regions – matrix and fracture domains.

The basic hydraulic functions; i.e. soil water retention curve  $\theta(h)$  and hydraulic conductivity function  $K(\theta)$  are analytically expressed according to van Genuchten (1980). The initial condition was set as  $h$  gradually changing from  $-500$  kPa at the top to  $-150$  kPa at the bottom of the soil profile. The top boundary condition was defined by hourly precipitation (including irrigation with the dye-solution) and calculated evapotranspiration. The bottom boundary condition was defined as free drainage.

## RESULTS AND DISCUSSION

### Distribution of the Brilliant Blue dye

Dye pattern profiles of particular CUTs, together with their dye coverages are documented in Fig. 4. Highly developed macropore systems within the whole pedon body of the experimental plot show high density of autonomous macropore structures, creating a mutually interconnected system. Nevertheless, some differences between the macropore structures are well visible. Within the CUT 2, macropore pathways are narrow and the top of CUT 2 profile is only slightly covered by BB dye. On the contrary, the top of CUT 24 soil profile is heavily covered with BB dye. In both, the CUT 24 and the CUT 27 profiles, the macropore pathways are broad, indicating increasing macropore-soil matrix interaction. The CUT 504 is different from the other CUTs, and finger-like structures are evident there.

The macropore structures presented in Fig. 4, have arisen due to the existence of structural voids with large apertures of geogenic origin, with minimal presence of biological channels. Due to well-developed periglacial (“cryogenic”) phenomena in the area, we propose that the macropores were formed by cycling of freezing and thawing events (Jury and Horton, 2004; Heller, 2012).

The dye coverage values ( $D_c$ ) as functions of the soil depth for the various  $1 \text{ m}^2$  cuts and their zoom in for the  $0.1 \text{ m}$  soil depth are presented in Figs.5a and 5b, respectively. The low  $D_c$  values in certain soil profiles indicate high fractions of the preferential flow, and high values of dye coverage indicate high fractions of the matrix flow. In CUT 2, the dye coverage value was small, from  $\sim 40\%$  to  $80\%$  at the top ( $0-0.1 \text{ m}$ ) soil layer (Figs. 5a and 5b), and then increased to  $\sim 80\%$  down to  $1 \text{ m}$  soil depth. In CUT 24, the dye coverage values were from  $\sim 80$  to  $100\%$  at the top soil layer and slightly decreased downward to  $\sim 80\%$ , and became similar to the values of CUT 2 at  $1 \text{ m}$  soil depth. These results indicate that during the time between 2 hours and 24 hours after the BB application there was an additional infiltration of the dye solution from the dye solution pool located at the top of the soil surface during the dye solution infiltration. In general, the  $D_c$  values at the top layer ( $0-0.1 \text{ m}$ ) in CUT 24, CUT 27, and CUT 504 were similar. However, these values were higher in CUT 27 and CUT 504 than in CUT 2 and CUT 24 in the  $\sim 0.3-0.6 \text{ m}$  soil layer. This fact can be explained by lateral dye solution redistribution in the  $\sim 0.3-0.6 \text{ m}$  soil layer during the time between 24 h to 504 h after the BB application, which caused the increase in the  $D_c$  values in CUT 27 and CUT 504 in this soil layer, and simultaneously, the remnant dye solution volume in this stage of dye solution redistribution was not able to increase the  $D_c$  values in the CUT 27 and the CUT 504 profiles in the  $\sim 0.7-1.0 \text{ m}$  soil layer.

The relative BB concentration values ( $C_{rel}$ ) as functions of soil depth for the various  $1 \text{ m}^2$  cuts are presented in Fig. 6. In comparison with Fig. 5, the most significant change in  $C_{rel}$  was observed in CUT 504 profile (Fig. 6), where the significant drop in  $C_{rel}$  was observed in depth  $0.0-0.5 \text{ m}$ . The drop in  $C_{rel}$  can be related to the impact of rain water invasion into the soil (Fig. 2) accompanied with the leaching of BB from the top and the middle part of the CUT 504 profile.

The proportions of SPW classes within the individual dye pattern profiles (Fig. 7) show that the growth of SPW category  $> 200 \text{ mm}$  from CUT 2 to CUT 504 profiles was accompanied by decrease in abundance of  $20-200 \text{ mm}$  SPW category. Small abundance of SPW category  $< 20 \text{ mm}$  and high abundance of SPW categories  $> 20 \text{ mm}$  and  $< 200 \text{ mm}$  are observed within the CUT 2 dye pattern profile, which reflects the growth of macropore – soil matrix interaction in time (macropore flow cession) and its gradual switch to the matrix dominated flow

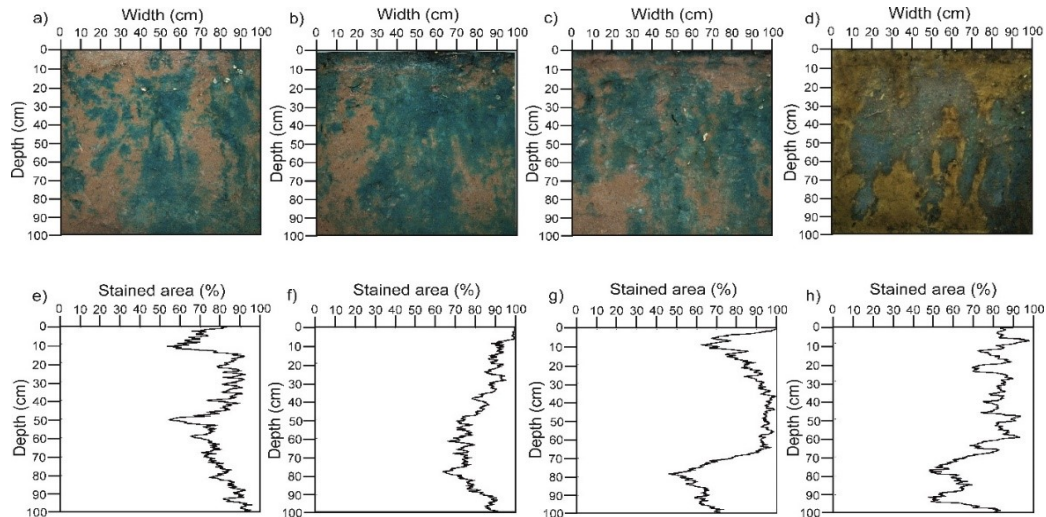


**Fig. 4.** Dye pattern profiles and corresponding dye pattern coverages (bottom) of CUT 2 (a), CUT 24 (b), CUT 27 (c) and CUT 504 (d) profiles (adapted from Bebej et al., 2017).

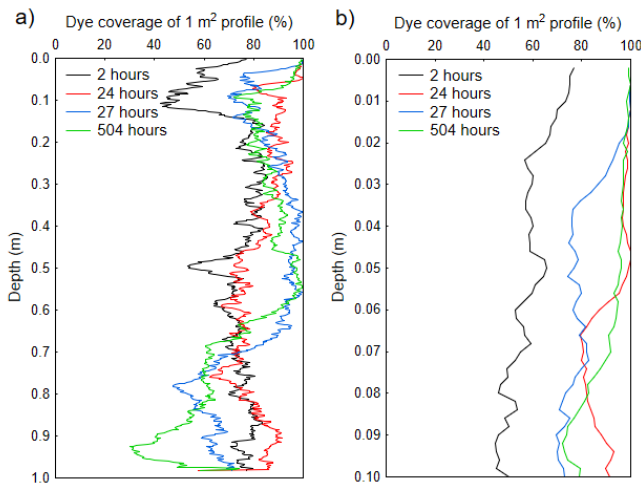


**Fig. 5.** a) Dye coverage profiles of CUT 2, CUT 24, CUT 27 and CUT 504, b) zoom of dye coverage in depth 0–0.1 m.

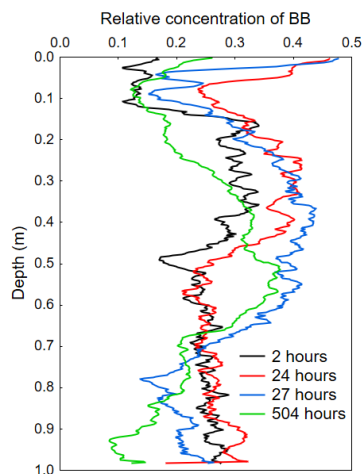


**Fig. 6.** The average concentration of BB in CUT 2 to CUT 504 soil profiles.

(corresponding also with the time of transition from infiltration to redistribution stage). Dominant abundance of SPW category > 200 mm within the CUT 24 –CUT 504 profiles indicate that

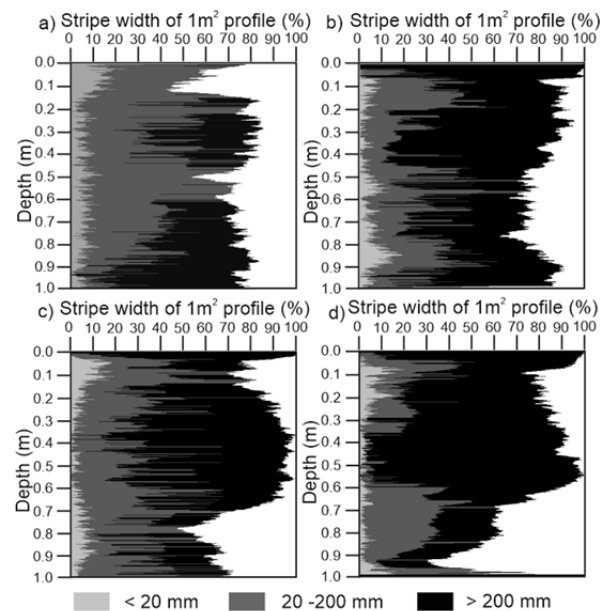


**Fig. 7.** Relative proportions of three SPW classes in the CUT 2 (a), CUT 24 (b) and CUT 27 (c), and CUT 504 soil profiles.

dye solution is entrapped within stained objects of high volume with small surface, visible in surface density profiles (Fig. 7). It should be noted that the SPW category <20 mm abundance is recorded in all analysed dye pattern profiles, but this SPW objects did not play a significant role in hydrological regime of dye solution during its redistribution in the soil pedon.

The top part of CUT 2 dye pattern profile (Fig. 7, a) provides important information about the initiation processes of macropore flow in the soil body. The low  $D_c$  value, as well as the presence of the SPW classes of both < 20 mm, and > 20 mm and < 200 mm, provide strong evidence that the macropore flow was initiated at the soil surface in the case of the experimental plot under investigation. By infiltration model of Weiler (2005), most of the macropores received very little water, while a few macropores received a large proportion of the total volume of dye solution irrigation water. It was proved that the total soil water content change in the soil matrix decreases with an increasing input rate, due to increased bypassing of the soil matrix (Weiler, 2005). This fact is strongly supported in this

study by both the SPW measurements and the dual permeability model simulation results, listed in Chapter 3.3. The other consequence resulting from the ratio of SPW of < 20 mm and > 200 mm classes documented for CUT 2 profile is that the macropore flow was a dominated process, which controlled infiltration of dye solution into the soil body in the time of CUT 2 dye pattern profile generation (Weiler and Flühler, 2004).

The distribution of SPW classes within the particular soil profile exposures enables to calculate flow type distribution (Fig. 8). According to Weiler and Flühler (2004) classification rule, only in the case of CUT 2 profile it is possible to document the abundance of macropore FTs, while in the other CUTs, matrix FTs are dominant (Fig. 8), or even the only FT within the dye pattern profile of CUT 24 is presented.

The surface area densities ( $S_v$ ) of stained objects in CUT 2 and CUT 24 profiles were very different from those of CUT 27 and CUT 504 (Fig. 9). In the case of CUT 2 profile, the  $S_v$  was large in those parts of the soil profile where the dye coverage profile (Fig. 5) reached its minimum. It is noticeable that the maximum  $S_v$  values were observed at the top of the CUT 2 profile, what indicates direct dye solution flow from the soil surface into the macropore pathways.

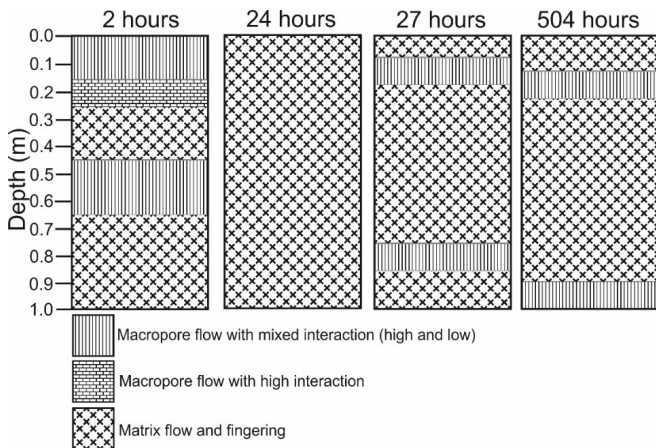


Fig. 8. Flow types categories observed in CUT 2 – CUT 504 profiles.

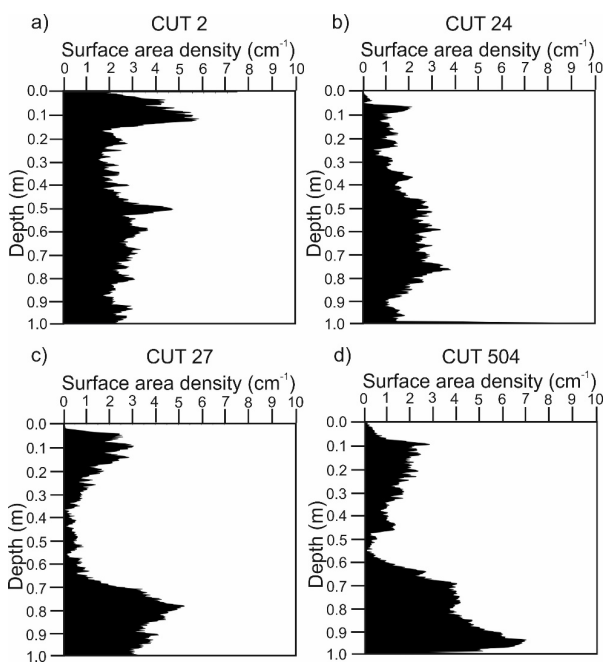


Fig. 9. The surface areal density profiles of vertical dye patterns of CUT 2–CUT 504 profiles.

In the case of the CUT 24 the process of  $S_v$  reduction (in comparison to CUT 2) is visible in the upper soil profile, what demonstrates the process of transition zone creation, with developing of matrix FTs, which can be linked with the infiltration of residual dye solution dosage from the surface of the experimental plot in the time between the CUT 2 and CUT 24 profile formations.

In the case of both the CUT 27 and the CUT 504 profiles the  $S_v$  started to grow at the upper part of the soil profile, where the dye coverage of profiles reached its local minimum (Fig. 5). The observed growth of  $S_v$  in these zones (as well as in the bottom part of the soil profiles, which was even more pronounced) indicates the turnover of the dye solution flow regime characterised by the existence of small stained objects with low volume but high surface density. The origin of high  $S_v$  values in the top part of the CUT 27 and CUT 504 profiles (Fig. 9) can be explained by finger propagation of the high-interaction zone, when the matric potential decreases behind the wetting front (Jury and Horton, 2004). In consequence, the SPW stained objects of both <20 mm and >20 mm and <200 mm dominate over >200 mm stained objects in the top parts of the CUT 27 and CUT 504 profiles (Fig. 7), and macropore FTs originated there due to emptying of >200 mm SPW objects (Jardine et al., 1990).

The massive growth of  $S_v$  observed in the bottom part of both the CUT 27 and the CUT 504 profiles is caused by a different mechanism than the one observed in the upper parts of the CUT 27 and the CUT 504 profiles. The SWC reached its maximum values in this depth (in contrast to the top parts of CUT 27 and CUT 504 profiles), while the  $D_c$  achieved its absolute minimum at these depths of CUT 504 (Fig. 5). Such a situation indicates minimal macropore-soil matrix interaction in deep zones with high volumetric skeleton content, which can be explained by drainage of residual dye solution from the horizons located above, via macropore PF pathways with domination of SPW objects <200 mm.

Fig. 10 summarises the obtained results and provides a general picture about the subsequent stages of dyed solution redistribution within the soil pedon, which are discussed in the following section.

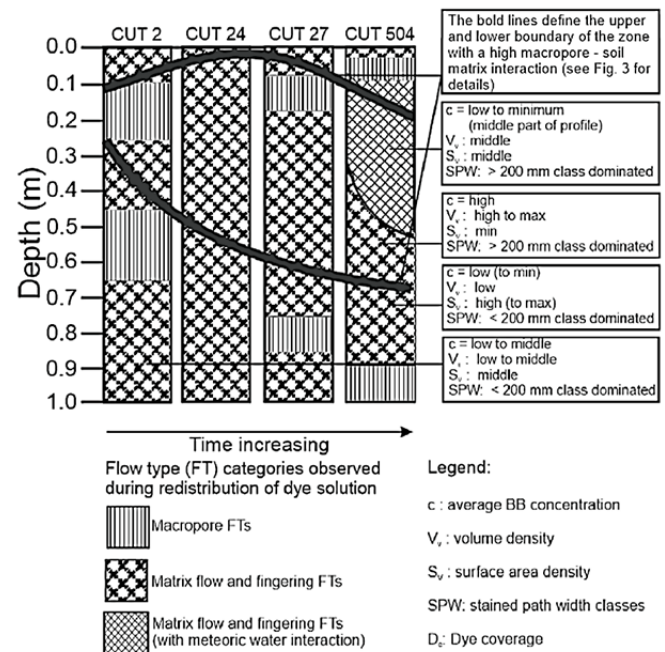


Fig. 10. The spatio-temporal distribution of flow type categories within the CUT 2 –CUT 504 profiles.

**Dual-permeability model simulations**

A dual permeability model provides the information about the SWC changes within both domains separately. It also calculates the actual and cumulative boundary fluxes on the top and bottom boundary of the modelling domain.

The results of water content profiles within the soil-matrix domain modelled with the simulation setup according to the description in the methodological chapter of this paper are shown in Fig. 11. The van Genuchten hydraulic parameters of both domains are listed in Table 2.

HYDRUS model simulates SWC profiles within the matrix domain quite well (Fig. 11). Since the SWC was measured by a gravimetric method on undisturbed soil samples, it must be

considered as the SWC of soil matrix only. Water within the fracture domain cannot be detected gravimetrically because of fracture-domain volume being void of water during the measurement. This is also the most probable reason for a slight overestimation of SWC in matrix domain by the model. The correlation between the measured and the simulated values of SWC is however very high. Still significant amount of (by time) unexplained variability should be ascribed to intrinsic spatial heterogeneity of the soil at the pedon scale (see  $R^2$  in Table 2). Anyway these results approve the dynamic interpretation of FT changes between the particular soil profiles exposed for different time lengths, since SWC profiles in all particular CUTs were successfully simulated with the same set-up of hydraulic parameters (Table 2).

**Table 2.** Hydraulic parameters of the porous system domains. ( $\theta_{s-m}$ ) is saturated soil water content of the matrix domain,  $\theta_{r-m}$  is a residual soil water content of the matrix domain,  $\alpha-m$  is a shape parameter of the matrix domain,  $n-m$  is a shape parameter of the matrix domain,  $K_{s-m}$  is saturated hydraulic conductivity of the matrix domain in  $cm\ h^{-1}$ ,  $\theta_{s-f}$  is saturated soil water content of the fracture domain,  $\theta_{r-f}$  is a residual soil water content of the fracture domain,  $\alpha-f$  is a shape parameter of the fracture domain,  $n-f$  is a shape parameter of the fracture domain,  $K_{s-f}$  is saturated hydraulic conductivity of the fracture domain in  $cm\ h^{-1}$ ,  $w$  is the ratio between macropore and matrix regions and measured (SWC-m) and simulated soil water contents (SWC-s) and  $\alpha_w$  is the mass transfer coefficient in  $cm^{-1}\ h^{-1}$ .

Hydraulic parameters		$\theta_{r-m}$	$\theta_{s-m}$	$\alpha-m$	$n-m$	$K_{s-m}$	$\theta_{r-f}$	$\theta_{s-f}$	$\alpha-f$	$n-f$	$K_{s-f}$	$w$	$\alpha_w$
Depth (cm)													
0-15		0.10	0.29	0.075	1.180	3.5	0.0	0.8	0.0124	2.0	300	0.2	2.42
15-30		0.16	0.29	0.061	1.120	10.0	0.0	0.8	0.0124	2.0	300	0.2	6.91
30-50		0.17	0.45	0.073	1.178	10.0	0.0	0.8	0.0124	2.0	300	0.2	6.91
50-90		0.12	0.45	0.068	1.150	10.0	0.0	0.8	0.0124	2.0	300	0.2	6.91
90-100		0.15	0.38	0.073	1.178	10.0	0.0	0.8	0.0124	2.0	300	0.2	6.91
CUTs/Depth (cm)		10 cm	20 cm	30 cm	40 cm	50 cm	60 cm	70 cm	80 cm	90 cm	100 cm		
CUT 2	SWC-measured (vol. %)	16.70	20.20	23.90	24.50	19.90	21.10	20.10	19.10	18.806	21.10		
	SWC-simulated (vol. %)	17.00	19.60	24.20	23.80	21.20	21.00	20.90	20.80	19.80	20.00		
	$R^2$						0.7924						
CUT 24	SWC-measured (vol. %)	16.00	19.40	21.10	23.60	20.60	20.80	18.50	19.10	17.60	18.90		
	SWC-simulated (vol. %)	16.80	19.90	24.00	25.20	24.70	22.30	22.10	22.00	21.80	20.40		
	$R^2$						0.6956						
CUT 27	SWC-measured (vol. %)	15.30	19.80	20.90	21.60	20.60	21.70	20.10	20.30	19.50	19.10		
	SWC-simulated (vol. %)	16.70	19.90	25.30	24.70	22.40	22.20	22.00	21.80	20.40	20.00		
	$R^2$						0.7464						
CUT 504	SWC-measured (vol. %)	14.50	15.10	18.00	17.90	20.40	20.30	20.80	21.10	21.00	19.60		
	SWC-simulated (vol. %)	14.60	15.00	21.10	24.20	24.40	23.00	23.10	23.20	21.70	21.90		
	$R^2$						0.7286						

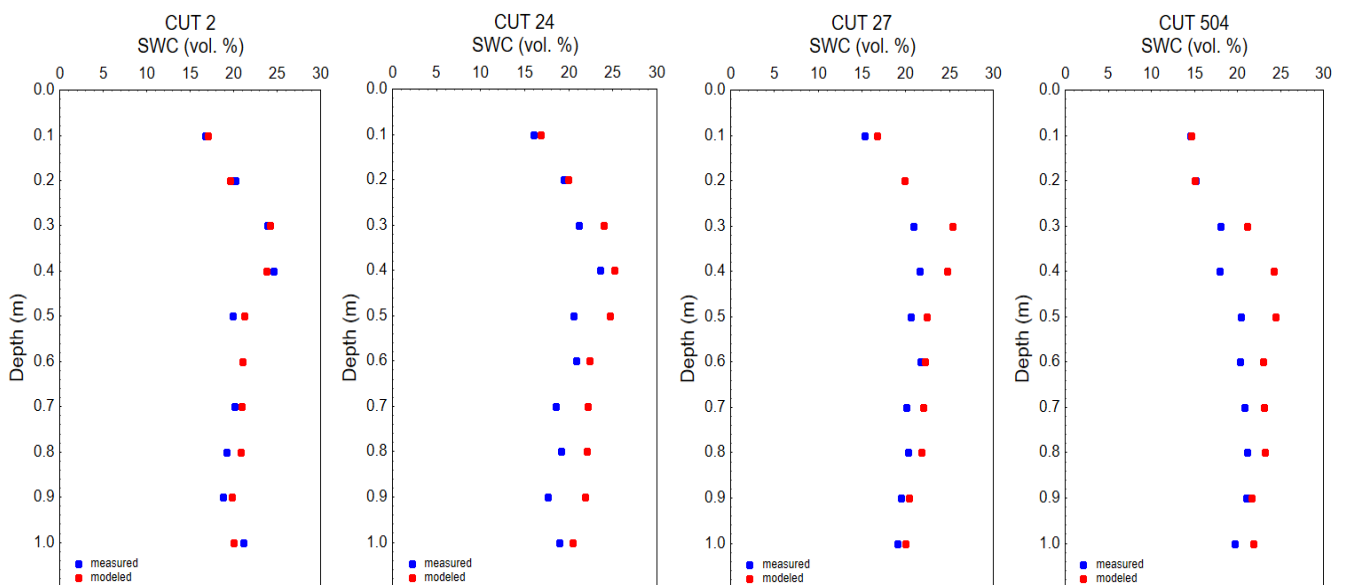


**Fig. 11.** Average values of measured and simulated (HYDRUS) of soil water content (SWC) within the particular CUT 2 (2-hour), CUT 24 (24-hour), CUT 27 (27-hour) and CUT 504 (504-hour) soil profiles.

The calibrated saturated water content of 0.8 for the fracture domain is relatively high but still a reasonable value (e.g. Gerke et al., 2013; Ireson et al., 2009; Kodešová 2017-personal communication; Mathias et al., 2006). The increase in matrix-domain SWC during the infiltration experiment is not substantial and is located only to particular depths of the soil profile.

From the (by HYDRUS) calculated water balance it follows that only some 30% of the irrigation water was utilised for the matrix SWC increase. The rest of the water either flowed out of the profile via large macropores (fracture domain) or it is actually present within the macropores. This was also supported by mathematical modelling, which shows the distribution of water between two domains and the amount of water which flowed out through the bottom boundary (Table 3).

**Table 3.** The average values of the SWC present within the particular soil domains (matrix and fractures) in particular times and the cumulative value of the flux through the bottom of soil pedon.

Time (hours)	SWC in matrix domain ( $\text{m}^3 \text{m}^{-3}$ )	SWC in fracture domain ( $\text{m}^3 \text{m}^{-3}$ )	Cumulative bottom flux ( $10^{-3} \text{ m}$ )
2	0.241	0.0702	10
24	0.22	0.025	50
27	0.22	0.024	51
504	0.22	0.013	110

## DISCUSSION

The hydropedological similarity concept used in this study does not mean the same as homogeneity and certainly some changes in porosity, bulk density or skeleton content are still affecting hydrological behaviour even within a single studied soil pedon (Fér et al., 2016; Moreira et al., 2016). Besides almost technical impossibility to make 2-D simulation of such a defined problem (section “Mathematical modelling of soil water content profiles”), also for this reason it was decided to simulate only horizontally averaged water contents within vertical soil profiles and compare them with SWC measured by the gravimetric method, which in fact avoids the fracture domain as the water drains from the largest pores yet immediately during the sampling process.

The variability of the dye coverage, surface density, SPW characteristics, as well as the BB concentration, provides information bases for the reconstruction of dye solution redistribution processes in soil pedon.

The dye flow processes within the experimental soil pedon started immediately after the beginning of irrigation, via macropore-flow pathways, recorded by macropore FTs in CUT 2 profile. Based on modelling with HYDRUS, the dye solution flow at this stage was really concentrated in fracture domain (about 60% of total dye solution applied). As the CUT 2 profile was excavated 2 hours after the completion of the sprinkling experiment, a certain amount of dye solution still remained at the soil surface, which afterwards saturated the top soil layer, as can be seen in CUT 24 profile (Fig. 5). At the same time, the matrix FT category of Weiler and Flühler (2004) began to emerge there (Fig. 8). The  $D_c$ ,  $C_{rel}$  values at the upper part of CUT 24 profile, as well as the SWC data recorded there indicate that the stage preceding the CUT 24 (dye pattern) profile creation, was characterised by maximum quantity of dye solution in this part of the soil profile.

When comparing the dye coverage ( $D_c$ ) in profiles of CUT 24 and CUT 27 with that of CUT 2, the growth of  $D_c$  values observed within the 0.1–0.6 m depth interval of CUT 24 - CUT

27 indicate the growth of macropore-soil matrix interaction, accompanied by the reduction of  $S_v$  values. This fact suggests that the dye solution was entrapped within the stained objects of > 20–200 mm with small  $S_v$  values typical for soil matrix environment. The comparison of both the shape and the overall geometry of CUT 24 - CUT 27  $D_c$  profiles document the subsidence of this macropore-soil matrix interaction zone into the deeper parts of the soil pedon.

The CUT 504 dye pattern profile manifests the impact of meteoric water on the ultimate dye pattern profile (Fig. 2). The intrusion of meteoric water caused the leaching of BB dye (Fig. 6), evident from the reduction of  $C_{rel}$  in the upper part of the CUT 504 profile.

The applied methodology of dye solution redistribution study, as well as the results obtained provide the evidences about the strong temporal control of dye solution flow within the analysed soil pedon. Fast changes were observed within few hours, what illustrates the remarkable dynamics of dye solution redistribution processes. On the other hand, the morphometric parameters of stained objects seemed to be sensitive enough to track these processes.

Bebej et al. (2017) have reported the physical-chemical changes caused by the application of Brilliant Blue dye (pH = 7) on acidic soils (pH < 4.0) from the same experiment. It was found that the application of BB dye solution abruptly increased the pH ( $\text{H}_2\text{O}$ ) values in all profiles (CUT 2-CUT 504) of the experimental plot, and that the comparison with REF profiles revealed the gradual drop in pH ( $\text{H}_2\text{O}$ ) from CUT 2 to CUT 504 profiles. Bebej et al. (2017) have documented also the changes of  $\text{Na}^+$  concentration ( $\text{cmol}_c \text{ kg}^{-1}$ ) in the soil exchangeable complex extracted from the zones of macropore PF of CUT 2 - CUT 504 profiles, analogous with those described for pH ( $\text{H}_2\text{O}$ ).

The obtained results are in line with the findings of Li and Ghodrati (1997), Weiler and Naef (2003) and Weiler (2005) who showed how a surface initiation process can generate extremely dynamic macropore flow.

Alaoui and Goetz (2008) presented dye tracer distribution in six soil profiles that were continuously excavated in steps of every 20 cm. The cited authors declared the soil profiles were excavated one day after irrigation, but unfortunately the reference about timing of individual vertical profile excavation is missing. Nevertheless, the morphometric parameters of the analysed dye objects showed many similarities with our experimental outputs: (i) the dye coverage gradually increased with time, and (ii) the concentration of BB dye increased with depth within the soil profile.

## CONCLUSIONS

The knowledge about the character of water redistribution within forest soils during extreme rainfalls or snow-melt situations is crucial for a set of practical applications, such as flood protection, silviculture, forest infrastructure management, etc. It has been proven that dye-tracer irrigation field experiments represent one of the suitable cost-effective tools to manifest and detect the local vadose zone hydrological processes, what is crucial for correct decisions in terms of above mentioned practical problems.

The presented case-study of the (dye solution) pedon-scale flow dynamics showed a key role of the time factor in succession of FTs observable via several vertical soil profiles excavated at different times.

Based on the numerical modelling, the time factor was able to explain from 70% up to 75% of the vertical variability of soil moisture profiles, which supports the assumption of hydropedological similarity of properly selected pedon-scale studies. Notwithstanding, the intrinsic 3-D heterogeneity of soil at the pedon scale may still embed a substantial portion of noise into 2-D result interpretations.

Three stages of dye solution redistribution processes were identified: (i) a stage of preferential macropore flow, (ii) a stage of strong interaction between macropore-domain and soil matrix leading to generation of heterogeneous matrix flow and fingering flow types, and (iii), a final stage of dye redistribution, which was predominantly connected with invasion of meteoric water into the soil pedon, resulting in substantial leaching of BB tracer from dye pattern profiles.

It was shown, how studies based on tracing of flow pathways in soil irrigated by dye solution can support the outputs of hydrological analyses. The question how the selected soil chemical properties (e.g., concentration of exchangeable cations) will reflect the observed spatiotemporal distribution of the dye tracer represents an interesting challenge for further research.

*Acknowledgement.* This work was supported by the Slovak Research and Development Agency under the contract No. APVV-15-0425 and the project of the scientific agency VEGA no. 2/0152/15. Part of the research was conducted under the project implementation: Centre of excellence for the integrated river basin management in the changing environmental conditions, ITMS code 26220120062; supported by the Research & Development Operational Programme funded by the ERDF.

## REFERENCES

- Alaoui, A., Goetz, B., 2008. Dye tracer and infiltration experiments to investigate macropore flow. *Geoderma*, 144, 279–286.
- Allaire, S.A., Roulier, S., Cessna, A.J., 2009. Quantifying preferential flow in soils: A review of different techniques. *J. Hydrol.*, 378, 179–204.
- Andrusov, D., Began, A., Biely, A., Borza, K., Buday, T., Bystrický, J., Bystrická, H., Cicha, I., Eliáš, M., Eliášová, H., Fusán, O., Gašparíková, V., Gross, P., Hanzlíková, E., Köhler, E., Houša, V., Lehotayová, R., Leško, B., Ložek, V., Menčík, E., Michalík, J., Mock, R., Pešl, V., Roth, Z., J., Samuel, O., Seneš, J., Slávik, J., Straník, Z., Špička, V., Vašíček, Z., Vaškovský, I., Vozár, J., 1985. *Stratigraphic Dictionary of Western Carpathians*. Vol. 2. Veda, Bratislava. (In Slovak.)
- Bargués Tobella, A., Reese, H., Almaw, A., Bayala, J., Malmer, A., Laudon, H., Ilstedt, A., 2014. The effect of trees on preferential flow and the soil infiltrability in an agroforestry parkland in semiarid Burkina Faso. *Water Resources Research*, 50, 4, 3342–3354.
- Bebej, J., Homolák, M., Orfánus, T., 2017. Interaction of Brilliant Blue dye solution with soil and its effect on mobility of compounds around the zones of preferential flows at spruce stand. *Cent. Eur. For. J.*, 63, 79–90.
- Beven, K., Germann, P., 1982. Macropores and water flow in soils. *Water Resources Research*, 18, 1311–1325.
- Bogner, CH., Borken, W., Huwe, B., 2012. Impact of preferential flow on soil chemistry of a podzol. *Geoderma*, 175–176, 37–56.
- Bundt, M., Widmer, F., Pesaro, M., Zeyer, J., Blaser, P., 2001. Preferential flow path: biological “hot spots” in soils. *Soil Biol. Biochem.*, 33, 729–738.
- Capuliak, J., Homolák, M., Aschenbrenner, Š., Ahmed, Y.A.R., Královič, R., 2008. Influence of litter on initial water transport in soil under forest stand. In: Šír, M., Tesáň, M., Lichner, E. (Eds.): *Hydrologie malého povodí*. ČVTS, Prague, pp. 59–66.
- Capuliak, J., Pichler, V., Flühler, H., Pichlerová, M., Homolák, M., 2010. Beech forest density control on the dominant water flow types in Andic soils. *Vadose Zone J.*, 9, 747–756.
- Droogers, P., Stein, A., Bouma, J., de Boer, G., 1998. Parameters for describing soil macroporosity derived from staining patterns. *Geoderma*, 83, 293–308.
- Fér, M., Leue, M., Kodešová, R., Gerke, H.H., Ellerbrock, R.H., 2016. Droplet infiltration dynamics and soil wettability related to soil organic matter of soil aggregate coatings and interiors. *J. Hydrol. Hydromech.*, 64, 2, 111–120.
- Forrer, I., Papritz, A., Kasteel, R., Flühler, H., Luca, D., 2000. Quantifying dye tracer in soil profiles by image processing. *Eur. J. Soil Sci.*, 51, 313–322.
- Flury, M., Flühler, H., 1994. Brilliant Blue FCF as a dye tracer for solute transport studies. A toxicological review. *J. Environ. Qual.*, 23, 1108–1112.
- Flury, M., Flühler, H., Jury, W.A., Leuenberger, J., 1994. Susceptibility of Soils to preferential Flow of Water. *Water Resour. Res.*, 30, 1945–1954.
- Garrido, F., Serrano, S., Barrios, L., Uruñuela, J., Helmhart, M., 2014. Preferential flow and metal distribution in a contaminated alluvial soil from São Domingos mine (Portugal). *Geoderma*, 213, 103–114.
- Gerke, H.H., 2006. Preferential flow descriptions for structured soils. *J. Plant Nutr. Soil Sci.*, 169, 382–400.
- Gerke, H.H., Dusek, J., Vogel, T., 2013. Solute mass transfer effects in two-dimensional dual-permeability modeling of bromide leaching from a tile-drained field. *Vadose Zone Journal* 12, 2, 1–21.
- Germán-Heins, J., Flury, M., 2000. Sorption of Brilliant Blue FCF in soils as affected by pH and ionic strength. *Geoderma*, 97, 1–2, 87–101.
- Ghodrati, M., Jury, W.A., 1990. A field study using dyes to characterize preferential flow of water. *Soil Sci. Soc. Am. J.*, 54, 1558–1563.
- Hagedorn, F., Bund, M., 2002. The age of preferential flow paths. *Geoderma*, 208, 119–132.
- Heller, K., 2012. Einfluss periglazialer Deckschichten auf die oberflächennahen Fließwege am Hang - eine Prozessstudie im Osterzgebirge, Sachsen. PhD Thesis. Technical University Dresden.
- Ireson, A.M., Mathias, S.S., Wheeler, H.S., Butler, A.P., Finch, J., 2009. A model for flow in the chalk unsaturated zone incorporating progressive weathering. *Journal of Hydrology*, 365, 244–260.
- IUSS Working Group WRB, 2015. World Reference Base for Soil Resources 2014, update 2015. International soil classification system for naming soils and creating legends for soil maps. World Soil Resources Reports No. 106. FAO, Rome.
- Jardine, P.M., Wilson, G.V., Luxmoore, R.J., 1990. Unsaturated solute transport through a forest soil during rain storm events. *Geoderma*, 46, 103–118.
- Jarvis, N.J., Dubus, I.G., 2006. State-of-the-art review on preferential flow. Report DL#6 of the FP6 EU-funded FOOT-PRINT project [www.eu-footprint.org], 60p.
- Jury, W.A., Horton, R., 2004. *Soil Physics*. 6<sup>th</sup> edition. John Wiley & Sons, Inc., Hoboken, New Jersey, USA.
- Kasteel, R., Vogel, H.J., Roth, R., 2002. Effect of non-linear

- adsorption on the transport behaviour of Brilliant Blue in a field soil. *Eur. J. Soil Sci.*, 53, 231–240.
- Kung, K.-J.S., 1990. Preferential flow in a sandy vadose zone. I. Field observation. *Geoderma*, 46, 51–58.
- Li, Y., Ghodrati, M., 1997. Preferential transport of solute transport through soil columns containing constructed macropores. *Soil Sci. Soc. Am. J.*, 61, 1308–1317.
- Mathias, S.A., Butler, A.P., Jackson, B.M., Wheeler, H.S., 2006. Transient simulations of flow and transport in the Chalk unsaturated zone. *Journal of Hydrology*, 330, 10–28.
- Mazúr, E., Lukniš, M., 1980. Geomorphologic Units Map 1:500 000. Atlas SSR. SÚGK, Bratislava. (In Slovak.)
- Moreira, P.H.S., van Genuchten, M.T., Orlande, H.R.B., Cotta, R.M., 2016. Bayesian estimation of the hydraulic and solute transport properties of a small-scale unsaturated soil column. *J. Hydrol. Hydromech.*, 64, 1, 30–44.
- Ohrstrom, P., Persson, M., Albergel, J., Zante, P., Nasri, S., Berndtsson, R., Olsson, J., 2002. Field-scale variation of preferential flow as indicated from dye coverage. *Journal of Hydrology*, 257, 164–173.
- Penman, H.L., 1948. Natural evaporation from open water, bare soil and grass. *Proceedings of the Royal Society*, A193, 120–146.
- Perret, J., Prasher, S.O., Kantzas, A., Langford, C., 1999. Three-dimensional quantification of macropore networks in undisturbed soil cores. *Soil Sci. Soc. Am. J.*, 63, 1530–1543.
- Ritsema, C.J., Dekker, L.W., 2000. Preferential flow in water repellent sandy soils: principles and modeling implications. *J. Hydrol.*, 231–232, 308–319.
- Shipitalo, M.J., Butt, K.R., 1999. Occupancy and geometrical properties of *Lumbricus terrestris* L. burrows affecting infiltration. *Pedobiologia*, 43, 782–794.
- Šimůnek, J., Jarvis, N.J., van Genuchten, M.T., Gärdenäs, A., 2003. Review comparison of models for describing non-equilibrium and preferential flow and transport in the vadose zone. *J. Hydrol.*, 272, 14–35.
- van Genuchten, M.T., 1980. A closed-form equation for predicting the hydraulic conductivity of unsaturated soils. *Soil Sci. Soc. Am. J.*, 44, 892–898.
- van Schaik, N.L.B.M., 2009. Spatial variability of infiltration patterns related to site characteristics in a semi-arid watershed. *Catena*, 78, 1, 36–47.
- Vogel, T., Lichner, L., Dusek, J., Cipakova, A., 2007. Dual-continuum analysis of a cadmium tracer field experiment. *Journal of Contaminant Hydrology*, 92, 50–65.
- Weiler, M.H., 2001. Mechanisms controlling macropore flow during infiltration. Dye tracer experiments and simulations. PhD Thesis. ETH Zurich.
- Weiler, M., 2005. An infiltration model based on flow variability in macropores: development, sensitivity analysis and applications. *J. Hydrol.*, 310, 294–315.
- Weiler, M., Flühler, H., 2004. Inferring flow types from dye patterns in macroporous soils. *Geoderma*, 120, 137–153.
- Weiler, M., Naef, F., 2003. Simulating surface and subsurface initiation of macropore flow. *J. Hydrol.*, 273, 139–154.
- Zehe, E., Flühler, H., 2001. Slope scale variation of flow patterns in soil profiles. *Journal of Hydrology*, 247, 116–132.

Received 29 September 2017

Accepted 5 April 2018